In vivo contribution of murine mesenchymal stem cells into multiple cell-types under minimal damage conditions

Fernando Anjos-Afonso, Elena K. Siapati and Dominique Bonnet*

Hematopoietic Stem Cell Laboratory, Cancer Research UK, London Research Institute, 44 Lincoln's Inn Fields, London, WC2A 3PX, UK
*Author for correspondence (e-mail: d.bonnet@cancer.org.uk)

Accepted 9 August 2004
Journal of Cell Science 117, 5655-5664 Published by The Company of Biologists 2004
doi:10.1242/jcs.01488

Summary

Murine mesenchymal stem cells are capable of differentiating in vitro into different lineages under stimulation with certain cytokines, growth factors and chemicals. However, the true capacitiy of these cells to contribute to different cell-types in vivo is still unclear, especially under minimal injury conditions. In this study, we describe a method of purifying murine mesenchymal stem cells from bone marrow and efficiently transducing them using a lentivirus vector expressing the eGFP reporter gene. Lentivirus-transduced mesenchymal stem cells retained their in vitro ability to differentiate into adipocytes, osteocytes and chondrocytes as well as into myocyte- and astrocyte-like cells. eGFP-mesenchymal stem cells were delivered systemically into minimally injured syngeneic mice. Tracking and tissue-specific differentiation were determined by PCR and immunohistochemistry, respectively. We found donor-derived hepatocytes, lung epithelial cells, myofibroblasts, myofibers and renal tubular cells in some of the recipient mice. Our data indicate that even in the absence of substantial injury, phenotypically defined murine mesenchymal stem cells could acquire tissue specific morphology and antigen expression and thus contribute to different tissue cell-types in vivo.

Key words: Mesenchymal, Stem, eGFP, In vivo, Differentiation

Introduction

Mesenchymal stem cells (MSCs) have the capacity to give rise to fat, bone and cartilage as well as to neuronal progenitors (Woodbury et al., 2000) and muscle (Wakitani et al., 1995) cells in vitro making them a potential cellular source for clinical applications in regenerative medicine. In vivo studies involving a variety of animal models have shown that MSCs may be useful in the repair or regeneration of damaged or mutated bone, cartilage, or myocardial tissues (Bianco and Robey, 2000; Pereira et al., 1998; Toma et al., 2002). They may also provide a useful tool for gene therapy strategies involving genes encoding secreted proteins (Bartholomew et al., 2001; Pereira et al., 1995; Duan et al., 2003). Although the in vitro differentiation capacities of MSCs have been well documented, the same potentials in contributing to different tissue cell-types in vivo remain elusive. So far, most in vivo studies have been performed by targeting a specific tissue/organ of interest, normally with the use of an injury model (Hofstetter et al., 2002; Kopen et al., 1999; Ortiz et al., 2003). Systemic delivery of MSCs is an attractive non-invasive strategy that allows repeated administration of large numbers of cells with great potential clinical applications (Bianco et al., 2001; Koc et al., 2002). However, limited data are available regarding the ultimate fate of systemically infused MSCs. In a baboon model, Devine et al. suggested that MSCs home to a variety of non-hematopoietic organs and may possess the capacity to proliferate within these tissues (Devine et al., 2003). Human MSCs (hMSCs) can differentiate into multiple cell types following peritoneal implantation in fetal sheep (Liechty et al., 2002). Using a partially purified murine MSC (muMSCs) population, Pereira et al. suggested that these cells follow a broad initial distribution and their presence could be detected in different tissues of the recipient animals a few months after transplantation without, however, exploring their in vivo differentiation potential (Pereira et al., 1995).

Therefore, the main aim of the present study was to test the efficacy of intravenous administration of a defined population of muMSCs. We evaluate their tissue distribution and 'natural' in vivo differentiation capacities in recipient animals not forced to undergo substantial organ degeneration first.

Most of the understanding of MSC biology has been acquired from studies on hMSCs. This is one of the uncommon situations when a cell type is better characterized in humans than in mouse. muMSCs are still poorly understood, in terms of their phenotype, cell isolation and expansion. Although mouse and human MSCs are generally similar in terms of overall phenotype and in vitro differentiation capacities, we present in this study that isolated and expanded muMSCs express different adhesion molecules and integrins compared with their human counterparts. Such discrepancies may account for and explain potential differences between human and mouse MSCs in homing and their in vivo capacity to contribute to specific cell-types (Liechty et al., 2002; Devine et al., 2003). Therefore, we considered it important to initially characterize these cells, reporting detailed and useful information about isolation, expansion and phenotype. Ex

vivo-expanded muMSCs were tagged by transduction with a lentiviral construct carrying the green fluorescent protein (eGFP) and, at various time points after infusion, multiple tissues were analyzed for the presence of the reporter gene by polymerase chain reaction (PCR). Immunohistochemistry was used to screen and determine any tissue-specific incorporation of donor-derived cells in the recipient animals.

We report that eGFP-MSCs showed variable distribution in different organs at 24 hours, with subsequent selective survival in some specific tissues for up to 4 weeks. Interestingly, MSCs were not able to home back to the bone marrow. Detailed screening of the presence of eGFP-MSCs revealed that most of these cells were only circulating and/or were trapped in different tissues (especially the lung) without being able to give rise to tissue specific cell-types at a significant level. However, we were able to identify, at a very low frequency, some tissue-specific cells expressing eGFP in the liver, kidney, muscle, connective tissue and lung. Despite the low incidence of this phenomenon, these findings indicate that muMSCs can give rise to different cell-types under minimal tissue damage conditions, suggesting that their in vitro multipotent properties may be shared in vivo.

Materials and Methods

Isolation, purification and expansion of MSCs

Bone marrow cells were collected by flushing the femurs, tibias and iliac crests from 8-12-week-old NOD/LtSz-scid/scid (NOD/SCID), NOD/SCID-β^{null} and C57BL6/J mice with PBS supplemented with 2% fetal bovine serum (FBS; Gibco, Paisley, UK). Red blood cell-depleted bone marrow mononuclear cells (BMMNCs) were plated at a density of 10^6 cells/cm^2 in murine mesenchymal medium with murine mesenchymal supplements (Stem Cell Technologies, Vancouver, Canada), further supplemented with 100 IU/ml penicillin and 100 μg/ml streptomycin (Gibco). Non-adherent cells were eliminated by a half medium change at day 3 and the whole medium was replaced weekly with fresh medium. The cells were grown for 2-3 weeks until attaining almost confluency. The whole adherent fraction was then detached by trypsinization and re-plated using a 1:3 dilution factor. Subsequent passing and seeding of the cells was performed at a density of 5000 cells/cm^2. The passage number of cultured (unpurified, Px or enriched, puPx) MSCs refers to the number of times that the cells had been trypsinized. To enrich MSCs, adherent cells from passage 2 (P2) and 3 (P3) were stained with rat anti-mouse CD45-CyChrome and CD11b-PE (BD Biosciences, Oxford, UK), or a combination of CD45 and biotin-conjugated lineage (Lin) cocktail antibodies (Stem Cell Technologies) followed by streptavidin-PE. The negative fraction from both cell surface antigens was sorted using the flow-activated sorter Vantage (Becton-Dickinson, Oxford, UK). Enriched MSC populations were cultured under the same conditions described above.

Colony forming units-fibroblast (CFU-F) assay

Red blood cell-depleted BMMNCs from NOD/SCID, NOD/SCID-β_2^{null} and C57B6/J mice were plated at a density of 5×10^5 cells/cm^2 and cultures were maintained as described above. At day 14, the medium was removed from the wells, washed twice with PBS and fixed with methanol. Giemsa stain was applied at room temperature for 5 minutes and colonies were counted microscopically.

Immunophenotyping of BMMNCs, cultured adherent cells and MSCs

Aliquots of freshly isolated BMMNCs from different mouse strains, unpurified and enriched MSC populations were phenotyped. All antibodies used in this study were purchased from Pharmingen unless otherwise stated. DAPI was used for exclusion of dead cells and analysis was performed using an LSR (Becton-Dickinson).

In vitro lentivirus-mediated gene (eGFP) transfer into MSCs

Transduction of MSCs was performed with an HIV-1-based self-inactivating (SIN) lentiviral vector (pHRSINcPPT-SEW), which carries the eGFP reporter gene under the control of the spleen focus-forming virus (SFFV) LTR (a kind gift from Prof. A. Thrasher, Institute of Child Health, London, UK). High titer viral stocks were obtained as previously described (Demaison et al., 2002). For transduction, 1×10^4 purified MSCs from passage 4 (purP4) were seeded into individual wells of a 12-well plate. The following day virus particles were added at multiplicity of infection (m.o.i.) of 5, 10, 30 or 50 and transduction was performed for 20 hours. Cells were harvested on day 1, 3 and 5 after virus removal and analyzed for eGFP expression by flow cytometry. eGFP-MSCs used for the in vivo studies were obtained using similar methodology, with cells from puP4 transduced at an m.o.i. of 50. Transduced cells were injected into mice 3-4 days after virus removal in order to reduce the number of cell passages used in our in vivo studies. To avoid viral contamination in the administered cell suspensions, transduced MSCs were washed several times with culture medium before cell infusion into mice.

In vitro culture differentiation conditions

eGFP-transduced MSCs were plated at a density of 2000 to 3000 cells/cm^2 in mesenchymal medium for 24 hours to 48 hours. After attachment, cells were washed once with basic differentiation medium, consisting of DMEM, 2% FBS and penicillin/streptomycin (all from Gibco), and then replaced with basic differentiation medium containing specific differentiation supplements. Osteogenic, adipogenic and chondrogenic supplements were described elsewhere (Pittenger et al., 1999). Myogenic differentiation was achieved by stimulating the cells with 10 μM 5-azacytidine and 5% horse serum (HS) (both from Sigma, Dorset, UK) for 24 hours (Wakitani et al., 1995); cultures were then maintained only with basic differentiation medium supplemented with 5% HS throughout the differentiation period. Astrocyte/neuronal induction supplements consisted of 50 ng/ml of basic fibroblast growth factor (bFGF) and 20 ng/ml of epidermal growth factor (EGF) (Peprotech, London, UK). Each specific differentiation medium was changed every 2-3 days and cultures were kept for 14 days with the exception of chondrogenic differentiation in which cells were incubated for 3 weeks.

Immunocytochemistry

Evaluation of osteogenic potential was performed by staining for alkaline phosphatase activity using an Alkaline Phosphatase Kit (Sigma) and calcium quantification using a Calcium Kit (Sigma) according to the manufacturer's recommendations. For adipogenic and chondrogenic determination, Oil Red O staining and Safranin O (Sigma) were used, respectively. For staining of astrocyte/neuronal and myogenic antigens, cells were fixed with 4% paraformaldehyde or methanol, permeabilized with 0.1% Triton-X, and stained with primary antibodies after blocking with 10% serum (rat and/or goat). TRITC or Cy3-coupled rat anti-mouse or goat anti-rabbit IgG secondary antibodies (Sigma) were used accordingly. Finally, slides were mounted with Vectashield (Vector Laboratories, Peterborough, UK) containing DAPI for nuclear staining. The anti-fast-twitch myosin (FTM) antibody was from Sigma while antibodies against Tau, GFAP and dystrophin were from Santa Cruz Biotechnology (Santa Cruz, CA). All primary and secondary antibodies were used at 1:200 and 1:400 dilutions, respectively, unless otherwise stated.

eGFP-MSCs infusion and detection of eGFP transgene by PCR

A total of 41 NOD/SCID mice aged between 8-12-weeks old were used in our two independent in vivo studies. All animal procedures were performed in accordance with our institutional guidelines. eGFP-MSCs (2×10^6), obtained a few days post-viral removal to minimize further expansion, were delivered intravenously (i.v.) by tail vein injection into each sublethally irradiated mouse (375 cGy using a ^{137}Cs source). Mice were then sacrificed on different days and specific tissues/organs collected. Genomic DNA was isolated from each tissue by lysis with buffer containing 1% SDS and 0.2 mg/ml Proteinase K (Sigma) followed by phenol-chloroform extraction. PCR conditions were 95°C 5 minutes, with 40 cycles of 95°C 45 minutes, 67°C 45 minutes and 72°C 45 minutes with the following primers: eGFP 5′-*caacagccacaacgtctatatcatg*/3′-*gaagttctaggcggtgttgta.* The integrity of the DNA samples was controlled by PCR for mouse GAPDH (5′-*cggagtcaacggatttggtcgtat*/3′-*agccttctccatggtggtgaagac*).

Tissue processing and immunohistochemistry

Tissues were fixed in 10% neutral buffered formaldehyde (NBF), embedded in paraffin and in some cases the other half of each tissue was cryo-embedded. Each embedded tissue was sectioned between 10 to 15 levels with a 70 to 100 μm gap between each one. Each level was serially sectioned at least 4 times. Sections (4 μm thick) were screened for the presence of eGFP either by staining with an eGFP antibody (Santa Cruz Biotechnology or an in house antibody, clone GFP 3E1; 1:100), or by direct visualization using a fluorescent microscope (Zeiss AxioVision2™, Zeiss, Welwyn Garden City, UK).

Paraffin sections were de-paraffinized, submitted to antigen retrieval (Vector Laboratories), and quenched for endogenous peroxidase (with 2% H_2O_2) and when necessary for endogenous alkaline phosphatase (with 20% acetic acid in methanol). Non-specific staining was blocked with 10% serum (rat and/or goat) and when biotinylated secondary antibodies (1:200) were used, endogenous biotin was blocked with the Biotin Blocking System Kit (Dako, Ely, UK). Cryosections (6 μm thick) were fixed with cold acetone and blocked with serum, and endogenous biotin was blocked when necessary. For light microscopy, immunoreactivity was detected using different peroxidase-based systems or alkaline phosphatase-based systems, or a combination of both (Vector Laboratories). For immunofluorescent staining, the secondary antibodies were Cy3- or TRITC-conjugated (Sigma). Antibody against desmin (1:80) was from Dako, α-smooth muscle actin (α-sma) and albumin were from Sigma; cytokeratin18 (CK18) and pan-cytokeratins (panCK) were from Santa Cruz Biotechnology. Lectins used were lycopersicon esculentum (1:100) from Sigma, and Lotus tetragonolobus (1:100) and Ricinus communis (1:100) from Vector Laboratories. Tissue and immunoglobulin isotype negative controls were included.

Results

Isolation and characterization of muMSCs

Since the ease of isolation and expansion of muMSCs is strain-dependent (Phinney et al., 1999; Peister et al., 2004), we initially used three different mouse strains (NOD/SCID, NOD/SCID-β^{null} and wild-type C57BL6/J) to determine the frequency of these cells in the bone marrow. muMSCs express a variety of cell surface antigens that are shared with different bone marrow-derived cell populations. As there is no specific antigen that can be used to directly define muMSCs in the bone marrow, we based our analysis on previous studies (Phinney et al., 1999; Peister et al., 2004). We have defined the murine mesenchymal compartment in the bone marrow as CD45$^-$Lin$^-$CD31$^-$ or CD45$^-$CD11b$^-$TER119$^-$CD31$^-$, which is the cellular fraction devoid of hematopoietic and endothelial cells (Fig. 1A). By using this criterion we have found no differences in the frequency of MSCs in the bone marrow of these mouse strains (Fig. 1A). Moreover, we did not see significant differences in the number of CFU-Fs with 1.66±0.38, 1.83±1.51 and 1.83±0.88 colonies/cm^2 obtained from NOD/SCID, NOD/

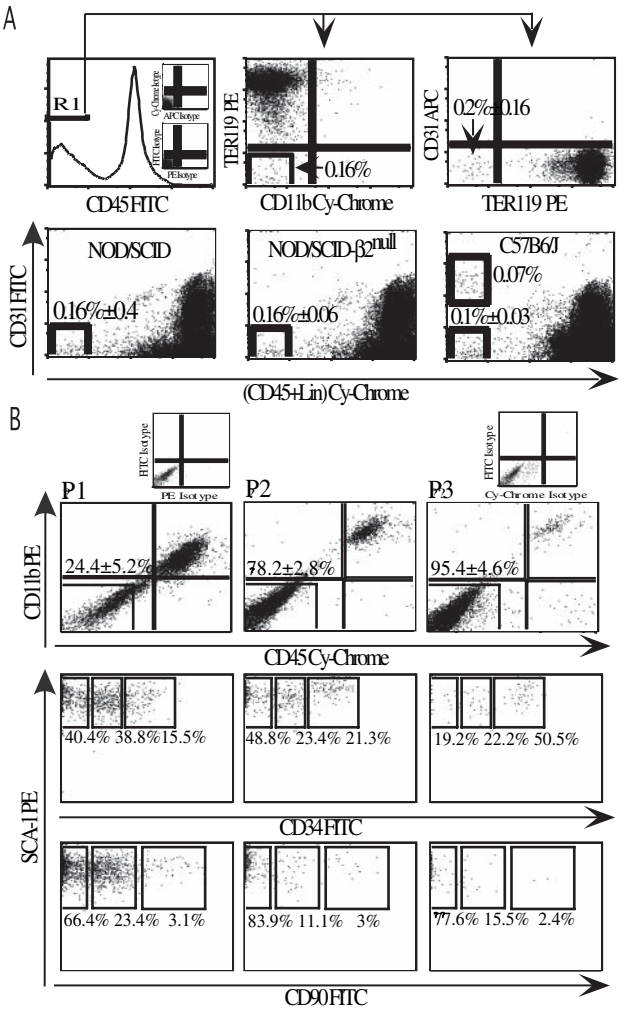

Fig. 1. Determination of muMSC frequency in the bone marrow (A) and persistence of hematopoietic cell contamination in MSC cultures (B). (A) Representative FACS plots analysis of NOD/SCID BMMNCs (top plots) stained with CD45/CD11b/TER119/CD31 antibodies; the frequency of muMSCs in the bone marrow can be considered as the negative fraction for CD45 (R1) with the combination of the other cell surface antigens used here. Alternatively, the same frequencies can also be determined by using the following antibody combination: CD45/Lin/CD31 (bottom plots). By using this criterion no differences in the frequency was found between the three mouse strains studied. (B) The presence of CD45$^+$/CD11b$^+$ cells in different passages (P1-P3) of MSC cultures is shown (top plots). Percentages indicate the CD45$^-$/CD11b$^-$ populations, which were considered as the MSC fraction. The CD45$^+$/11b$^+$ hematopoietic cell population expressed SCA-1 and different levels of CD34 and CD90 (middle and bottom plots, respectively). Results shown are mean±s.d from three independent experiments.

SCID-β_2^{null} and C57B6/J BMMNCs, respectively (±s.d from two independent experiments, each one performed in triplicate). However, MSCs from the immunodeficient strains exhibited more independence from the hematopoietic contaminants for its survival in early passages (F. Anjos-Afonso, unpublished). Therefore, muMSCs from the immunodeficient strains exhibited higher cell expansion and survival potential after removal of the hematopoietic cells than those from the wild-type C57Bl/6J strain. Thus, all subsequent experiments were conducted using NOD/SCID bone marrow.

As previously reported (Phinney et al., 1999), we observed that MSC cultures were contaminated with hematopoietic cells co-expressing CD45 and CD11b, which persisted for many passages (Fig. 1B). Contaminating cells consisted of 0.5-2% B cells ($CD19^+$), T cells ($CD3^+$), NK cells ($NK1.1^+$) and granulocytes ($Ly\text{-}6Gr^+$) (data not shown) but, interestingly, the majority of the persisting adherent $CD45^+/11b^+$ cells had a more progenitor/stem cell phenotype expressing a combination of stem cell antigens such as SCA-1, CD34 and CD90 (Fig. 1B). No $Ter119^+$ or $CD31^+$ cells were found after the first passage (data not shown) suggesting that CD45 and CD11b markers could be safely used as a routine method for purifying MSCs. In addition, we found that SCA-1 expression on MSCs increased from 42±11% (P0), to 44±10.9% (P1), 81.7±12.9% (P2) and finally to >98.5% on passage 3, indicating a possible acquisition of this antigen through time in culture. Alternatively, $SCA\text{-}1^+$ cells may have a selective advantage in our culture conditions.

After purification (>99.8% purity by FACS), MSCs were immunophenotyped by FACS analysis to reveal the expression of stem cell antigens such as CD34 and SCA-1 but not CD90. Moreover, the cells expressed CD9, CD29, CD44, CD73 and CD105. Importantly, MSCs weakly expressed or were negative for antigens that play an important role in homing/rolling/attachment such as ICAM-1, ICAM-2, E-selectin, P-selectin, VLA-5 and VCAM-1 (Table 1). Again, these important antigens are found be expressed on human MSCs (Deans and Moseley, 2000) (F. Anjos-Afonso, unpublished).

Table 1. Immunophenotype of muMSCs

Common name	CD	Detection
Hematopoietic antigens		
LFA-3L	CD2	Neg
CD3 complex	CD3e	Neg
T4 cell	CD4	Neg
Ly-1	CD5	Neg
T8 cell	CD8	Neg
LSP-R	CD14	Neg
B cell antigen	CD19	Neg
	CD34	Pos (++)
Leukosialin	CD43	Neg
Leukocyte common antigen	CD45	Neg
	CD45/B220	Neg
NK cell antigen	NK1.1	Neg
Erythroid antigen	TER119	Neg
Granulocyte antigen	Ly-6G	Neg
Thy-1	CD90	Neg
Stem cell antigen	SCA-1	Pos (+++)
Early B lineage antigen	AA4.1	Neg
Adhesion molecules		
ICAM-1	CD54	(+/–)
ICAM-2	CD103	Pos (+)
L-selectin	CD62L	Pos (+)
E-selectin	CD62E	Neg
P-selectin	CD62P	Neg
PECAM-1	CD31	Neg
HCAM	CD44	Pos (+++)
VCAM-1	CD106	Pos (+)
MadCAM-1	MadCAM-1	(+/–)
Integrins		
LFA-1 α chain	CD11a	Neg
Mac1	CD11b	Neg
CR4 α chain	CD11c	Pos (+)
VLA-4	CD49e	Neg
VLA-5	CD49e	Pos (+)
VLA-β1 chain	CD29	Pos (++)
Integrin αIEL Chain	CD103	Neg
Integrin β7 chain	β7	Neg
LPAM-1	α4β7	Neg
Cytokine receptors		
IL2-R	CD25	Neg
IL7-R	CD127	Pos (+/–)
c-Kit	CD117	Neg
Flk-2/Flk-3	CD135	Neg
Others		
Ecto-5′-nucleotidase	CD73	Pos (++)
Endoglin	CD105	Pos (+)
Tetraspan	CD9	Pos (+++)
MHC I	$H\text{-}2K^d$	Pos (+++)
MHC II	$I\text{-}Ag^7$	Pos (+)

muMSCs were analyzed by FACS with a panel of antibodies using isotype controls to set up the initial gates. Depending on the mean fluorescence intensity levels observed, samples were scored as negative (Neg), positive (Pos), borderline (+/–), low positive (+), fairly positive (++) or highly positive (+++).

MSCs can be efficiently transduced with eGFP-lentivirus vector without losing their in vitro differentiation capacities

After obtaining an enriched MSC population (purP4), we transduced the cells with an HIV-1-based lentivirus vector carrying the eGFP reporter gene. Transduction conditions were optimized by using different multiplicities of infection (m.o.i. 5-50) and the transduction efficiency was analyzed by FACS for eGFP. Efficient eGFP expression was observed as soon as one day after removal of the virus supernatant (Fig. 2A). The highest transduction efficiency (>98%) was achieved when an m.o.i. of 50 was used and this expression was maintained days after virus removal (Fig. 2B, 5 days post-virus removal). The percentage of eGFP-expressing cells remained virtually unchanged (>96.5%) in subsequent passages (purP4 to purP10), which correlated to 35 to 40 days post-transduction. This also indicated that the SFFV promoter was not subject to reporter gene silencing in these cells. To evaluate whether lentiviral transduction altered the differentiation properties of MSCs in vitro, we stimulated the transduced cells to differentiate into several cell-types. In vitro differentiation studies showed that eGFP-MSCs could give rise to different lineages (Fig. 3) such as adipocytes, which were visualized with Oil Red O staining (Fig. 3B,C). Chondrogenic capacity was confirmed with Alirezin-red, Alcian-blue (data not shown) and Safranin O (Fig. 3E) staining indicating the presence of sulfated proteoglycans in the micro-pellet formation. The differentiation into osteocytes was revealed using staining for alkaline phosphatase and calcium production (Fig. 3F,G). eGFP-MSCs were also able to give rise to myocytes with the

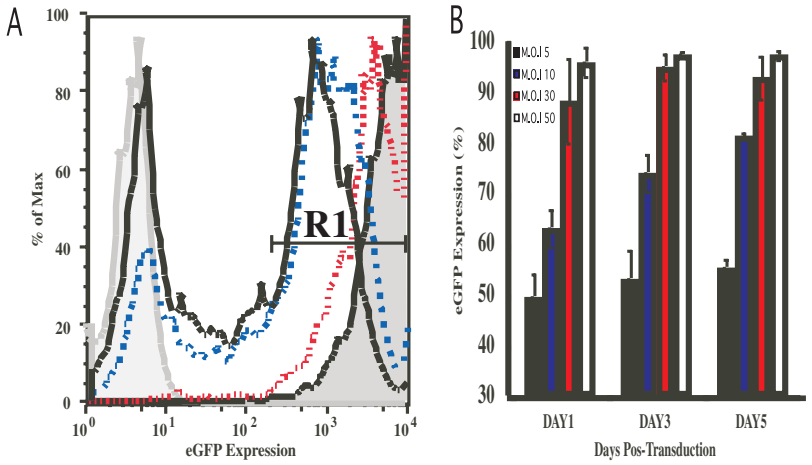

Fig. 2. In vitro eGFP expression by muMSCs following lentiviral transduction. A purified highly enriched muMSC population (puP4) was transduced with lentivirus for 20 hours. Analysis for eGFP expression was performed 1, 3 and 5 days post-transduction. (A) A representative overlay FACS plot from day 1 with m.o.i.=5 (solid line), 10 (blue dotted line), 30 (red dashed line), 50 (dark grey area) and untransduced control MSCs (light grey area) is shown. Cells gated in R1 expressing high levels of eGFP from different time points of analysis were plotted in the graph (B). Results shown are mean±s.d. from two independent experiments, and each time point was performed in duplicate.

expression of dystrophin, and fast-twitch myosin (Fig. 3H-K) and astrocytes/neuronal–like cells with the expression of GFAP and Tau (Fig. 3L-O). Additionally, expression of eGFP was maintained throughout the in vitro differentiation of these cells, indicating again that the SFFV promoter was functional after in vitro stimulation. We therefore used eGFP as a means of tracking muMSCs following in vivo administration.

Distribution of highly transduced eGFP-MSCs into different tissues

eGFP-MSCs were injected intravenously into syngeneic mice that had been sublethally irradiated simply to prime the bone marrow for homing of infused cells. However, sublethal irradiation (at the dose of 375 cGy used here) is a non-invasive method known to also cause minor damage to the gut and lungs. We used PCR analysis for eGFP to qualitatively evaluate the distribution of the transduced donor-derived cells in different tissues of the recipient animals (Table 2). We followed the distribution of the infused cells from day 1 to 28 post-transplantation. Surprisingly, we could not detect these cells in the bone marrow, indicating a deficient capacity of muMSCs to home to their tissue of origin (also confirmed by FACS analysis). We believe that the lack of appropriate adhesion molecules and integrins have impeded these cells to home and seed the bone marrow properly. Our data differ from what is known about the homing capacity of hMSCs to the bone marrow (Liechty et al., 2002; Devine et al., 2003) suggesting that there may be some in vivo functional differences between mouse and human MSCs.

PCR analysis showed that the lungs, liver and kidney were the primary resident organs of muMSCs, as eGFP could be detected as early as one day post-transplantation. Distribution to the muscle, heart, brain and spleen did not occur until day 7 after infusion. The fact that eGFP-MSCs were found circulating in the peripheral blood at all the time-points may explain why we were able to detect the reporter gene abundantly in many tissues by PCR while by immunohistochemistry low or no eGFP-positive cells were detected that had differentiated into other cell types. Therefore, quantification of the PCR data would not necessarily correlate with muMSC differentiation events but will most likely represent the extent of circulating cells in the respective tissues.

Extensive trapping of muMSCs especially in the lung

An adverse effect observed in the majority of the experimental animals transplanted with eGFP-MSCs was retention of these cells in the lung alveoli. Aggregates of MSCs were observed in the lung as early as one day post-transplantation and in many cases persisted thereafter to result in tissue damage with development of fibrotic tissue (with cysts containing collagen deposition) as well as impaired organ function (Fig. 4C,F). These animals exhibited distress, with gradual weight loss and

Table 2. Percentage of mice that were positive for eGFP in different tissues detected by PCR

Brain	0% (0/6)	0% (0/7)	14% (1/7)	20% (1/5)	8% (1/13)
Gut	17% (1/6)	0% (0/6)	43% (3/7)	17% (1/6)	62% (8/13)
Liver	57% (4/7)	17% (1/7)	43% (3/7)	33% (2/6)	69% (9/13)
Lung	83% (5/6)	17% (1/7)	17% (1/7)	60% (3/5)	54% (7/13)
Kidney	43% (3/7)	17% (1/7)	43% (3/7)	43% (3/7)	50% (6/12)
Skin	29% (2/7)	0% (0/7)	0% (0/5)	25% (1/5)	54% (7/13)
Muscle	0% (0/6)	0% (0/6)	17% (1/7)	17% (1/6)	8% (1/13)
Heart	0% (0/7)	0% (0/7)	29% (2/7)	33% (2/6)	8% (1/13)
Spleen	0% (0/6)	0% (0/6)	40% (2/5)	43% (3/7)	46% (6/13)
Bone marrow	0% (0/3)	0% (0/1)	–	0% (0/4)	0% (0/5)
Peripheral blood	25% (1/4)	33% (1/3)	25% (1/4)	60% (3/5)	60% (6/10)
Days post-infusion	1	2	7	14	28

Different tissues/organs were collected at various time points (day 1, 2, 7, 14 and 28) after infusion of eGFP-MSCs into sublethally irradiated recipients. DNA was extracted from these tissues and analyzed for the presence of the reporter gene by PCR. Numbers shown indicate mice positive for eGFP over total number of mice analyzed. (–) Not performed.

breathing difficulties and, therefore, had to be sacrificed. Immunohistochemistry performed on tissues where trapped eGFP-MSCs had been observed (e.g. spleen, lungs, and gut) revealed that these cells maintained their MSC phenotype by expressing laminin and endoglin (data not shown). Lungs extensively infiltrated with infused cells did not show reliable staining for lung-specific antigens such as lectin lycopersicon esculentum (Fig. 4D), pan-CK or surfactant protein C (data not shown), due to the extent of tissue damage.

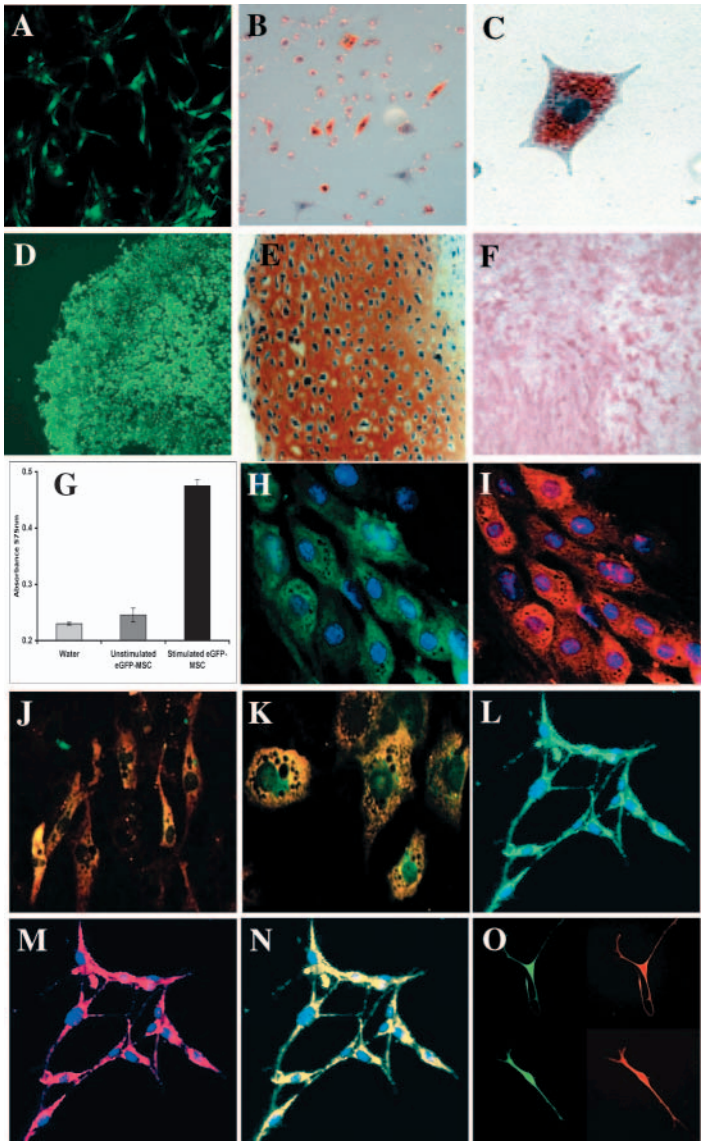

Fig. 3. In vitro differentiation of eGFP-MSCs. Unstimulated eGFP-MSCs were viewed under UV light (A). After 14 days of induction, cells were fixed and stained with Oil Red O (B,C). Chondrogenic differentiation was revealed with Safranin O staining (E) with a representative section of the micropellet viewed under the fluorescent microscope before the staining (D). The osteogenic potential of MSCs was determined by staining for alkaline-phosphatase (F) and calcium production (G): stimulated eGFP-MSCs (black bar), non-stimulated eGFP-MSCs (grey bar), control-water (light grey bar). Results shown are mean±s.d. from two independent experiments, each one performed in triplicate. eGFP expression alone on myocyte-like cells (H). Myogenic differentiation was confirmed by staining with dystrophin-Cy3 (I,J) and FTM-Cy3 (K). eGFP expression alone on astrocyte- (L) and neuronal-like (O) cells. Neuronal differentiation was confirmed by staining with GFAP-Cy3 (M,N) and Tau-TRITC (O). Overlay of eGFP and dystrophin (J), eGFP and FTM (K) and eGFP with GFAP (N). Cells were counterstained with hematoxylin (B,C,F), DAPI (H-J, L-N) or methyl green (E). Magnifications: ×100 (A,B,F); ×200 (D,L-N); ×400 (C,E,H-K,O).

Contribution of eGFP-MSCs to different tissue cell-types at low frequency

Tissues were subsequently screened for the presence of eGFP-MSCs focusing on the last time point (day 28) for the detection of differentiation events by immunohistochemistry. In order to avoid any false positive results, we validated positive event(s) only when we could detect $eGFP^+$ cells in the adjacent serial sections and when more than one $eGFP^+$ cell could be found on different levels of sections within a particular tissue. Isotype control antibody for eGFP was also used to exclude non-specific staining.

In two animals in which no lung damage was observed, we detected some $eGFP^+$ MSCs (Fig. 5A3) that had given rise to cells with respiratory bronchiolar epithelial

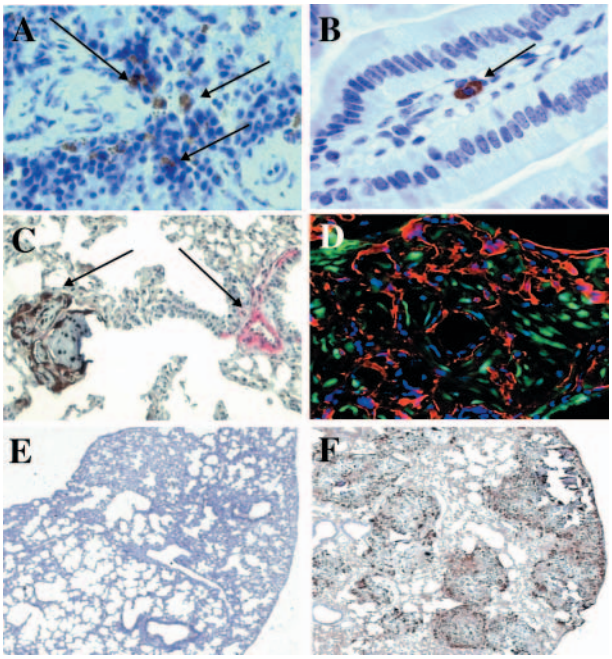

Fig. 4. Transplanted eGFP-MSCs are circulating and/or trapped in the different tissues. Immnunohistochemistry revealed the presence of infused eGFP-MSCs in different tissues. Circulating or trapped (arrows to brown cells) MSCs were found in the spleen (A), gut (B) and lung (C). In the lung, trapped cells stained neither for α-sma [(red-pink) indicated by the right-hand arrow] (C) nor for the lectin Lycopersicon esculentum-Cy3 (D, overlay with eGFP). Trapped eGFP-MSCs have caused severe lung damage in some of the mice. Representative sections of an undamaged lung (E) and severely damaged lung (F) from two different mice that were injected with eGFP-MSCs (brown cells) are shown. Sections were counterstained with hematoxylin (A-C,E,F) or DAPI (D). Magnifications: ×25 (E,F); ×100 (C); ×200 (D); ×400 (A,B).

morphology, staining positive with pan-CK antibody (Fig. 5A4).

We were able to detect eGFP-expressing cells with hepatocyte morphology in the liver of 3 out of 13 recipient animals. This was a low frequency event and in most cases only 1 to 3 positive cells were seen per section, suggesting that no or little cell expansion had occurred after the cells reached the liver. Interestingly, all positive cells were found near or not far from the blood vessels. These eGFP$^+$ cells had not only acquired proper hepatocyte morphology (Fig. 5B1,2,4) but also stained positive for specific antigens such as albumin (Fig. 5B2) and CK18 (Fig. 5B4).

In addition, specific eGFP$^+$ cells were observed in the kidneys of 2 out of 13 mice analyzed. These cells had renal tubular cell morphology and were seen at a frequency of 5-10 cells per section as well as on different levels of the tissue (Fig. 5C2,3,5). Immunohistochemistry on serial sections was performed to confirm expression of kidney-specific antigens by these eGFP-expressing cells. Indeed, these donor-derived cells stained positive for lectins such as ricinus communis or lotus tetragonolobus (Fig. 5C2,4, respectively).

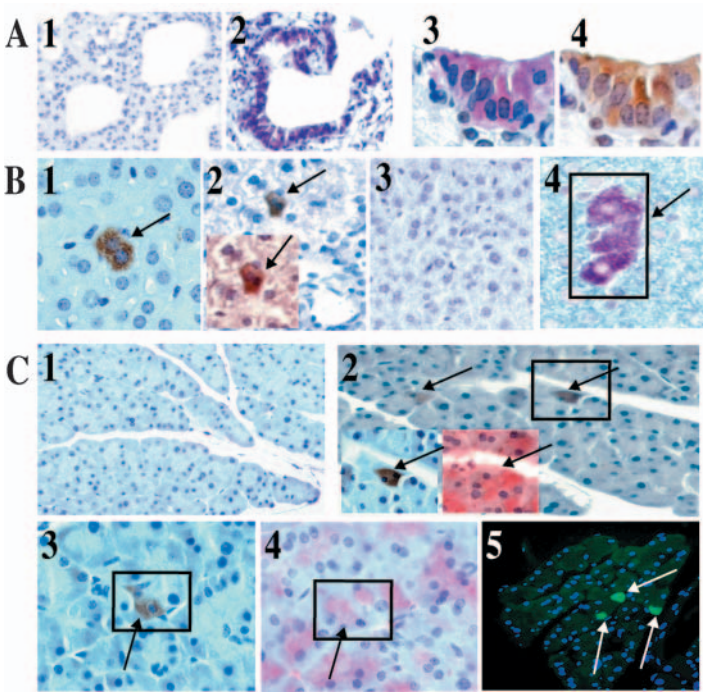

Fig. 5. In vivo contribution of eGFP-MSCs into bronchiolar epithelial, hepatocyte and renal tubular-like cells. (A) Representative paraffin sections of lung stained either with rabbit immunoglobulins (isotype control) (A1) or with rabbit anti-pan-CK antibodies (A2). Serial sections (A3,4) show that a group of pan-CK+ cells (red) (A4) also stained positive for eGFP (A3). (B) Representative liver sections with hepatocytes staining positive for eGFP (B1,2; brown). eGFP expression coincided with albumin (red) giving a brown-purple staining (B2, inset). Serial paraffin sections from another liver showing purple cells with hepatocyte morphology, as a result of co-expression of eGFP (red) and CK18 (blue) (B4). Isotype control sections shown in B3. (C) Differentiation of eGFP-MSCs into renal tubular cells. Paraffin-embedded sections stained with isotype control antibodies show no background staining (C1). Arrows indicate eGFP$^+$ cells after staining with rabbit anti-eGFP antibody (C2,3) co-expressing both lectins Ricinus communis (C2, bottom-center inset; red staining) and Lotus tetragonolobus (C4; pink-red staining) as shown in serial sections. A frozen section of a kidney demonstrating eGFP$^+$ cells by direct visualization using a fluorescent microscope (C5). All sections were counterstained with hematoxylin (except for B4) or DAPI (C5). Magnifications: ×100 (A1,2); ×200 (C1,2,5); ×400 (A3,4, B1-4, C3,4).

Since muMSCs were previously shown to have the capacity to differentiate into skeletal muscle in an injury model (De Bari et al., 2003) we also looked in more detail at this particular tissue for the presence of donor-derived cells. We could not find any eGFP$^+$ myofibers from skeletal muscle isolated from the femur of recipient animals. However, we found infiltrating eGFP$^+$ cells that had acquired myofibroblast-like morphology in the skeletal muscle (Fig. 6A1,4). These cells were found among myofibers, structurally resembled connective tissue and had acquired expression of α-sma (Fig. 6A5,6) but not desmin (Fig. 6A2,3) or FTM (data not shown). It has been previously reported that some stromal cells express α-sma (Peled et al., 1991). However, this antigen was undetectable in the MSC population before injection and the trapped cells in the lung did not acquire the expression of α-sma (Fig. 4C). Therefore, our data suggest that the expression of α-sma was an acquisition through a possible change in phenotype of the infused MSCs into a supporting-like tissue within the muscle fibers. Despite the large infiltration of these myofibroblast-like cells, no apparent muscle impairment was observed in these mice. We also investigated the muscle of the ears of these animals. We found eGFP$^+$ cells in 2 out of 13 mice (Fig. 6B2,3). These cells exhibited a myofiber morphology and expressed desmin (Fig. 6B4,5) and FTM (Fig. 6B6,7), indicating an acquisition of a myofiber-like phenotype. Interestingly, these eGFP+ cells formed clusters of 3-5 cells, each suggesting a possible expansion of donor-derived cells. Of course we cannot rule out the possibility that eGFP-MSCs fused with existing myofibers. The difference observed here among the two skeletal muscle regions is in agreement with recent reports indicating significantly different incorporation of bone marrow-derived cells among skeletal muscles (Brazelton et al., 2003).

In conclusion, we describe multiple incorporation events of muMSCs into the recipient tissues followed by systemic infusion under substantial tissue damage conditions.

Discussion

Reports in the literature have so far given a rather confusing concept about the in vivo contribution potential of MSCs. Firstly, the majority of the studies have used an undefined population of bone marrow cells making it unclear whether these properties are of mesenchymal or hematopoietic origin. This is of vital importance as hematopoietic stem cells have initially been shown to differentiate into hepatocytes (Lagasse et al., 2000), cardiomyocytes (Jackson et al., 2001), Purkinje neurons (Wagers et al., 2002), renal tubular cells (Kale et al., 2003), or even give rise to multiple tissues (Krause et al., 2001) in vivo.

It is very important to define an enriched MSC population before addressing the differentiation capacities of muMSCs. This is further emphasized by the observation that the adherent fraction of mouse bone marrow

mononuclear cells contains hematopoietic cells, which can persist after several passages (Phinney et al., 1999; Baddoo et al., 2003). Here, we confirm this finding, and further indicate that a high proportion of these contaminating hematopoietic cells have a progenitor/stem cell phenotype. By using CD45 and CD11b we were able to define and sort a highly enriched population of muMSCs that were devoid of hematopoietic cell contamination and could be efficiently transduced with a lentivirus vector. Moreover, the SFFV promoter in this construct retained the reporter gene expression through in vitro differentiation of muMSCs, indicating that it is functional in different cell lineages and could be utilized in gene therapy applications using MSCs.

So far, there have been no conclusive reports illustrating the in vivo contribution of muMSCs to multiple cell-types upon intravenous delivery without severe tissue damage being applied to the recipient animals. Only when injury models (Gojo et al., 2003) were used and MSCs were locally delivered, the differentiation potentials of these cells were observed. Nevertheless, muMSCs can specifically differentiate into astrocytes (Kopen et al., 1999) and type II pneumocytes (Ortiz et al., 2003) when injected directly into the spinal cord, brain or delivered into the lungs, respectively. Multilineage differentiation of murine MSCs has been observed only in the case of murine multipotent adult progenitor cells (MAPCs). These cells were shown to differentiate into hematopoietic cells in the marrow, blood, spleen, as well as into various tissue cell types after i.v administration (Jiang et al., 2002). However, it remains to be determined whether MAPCs exist as such in vivo or are a consequence of de-differentiation of an MSC-like cell, which might have emerged from a specific and selective culture system, giving rise to a unique in vitro phenotype.

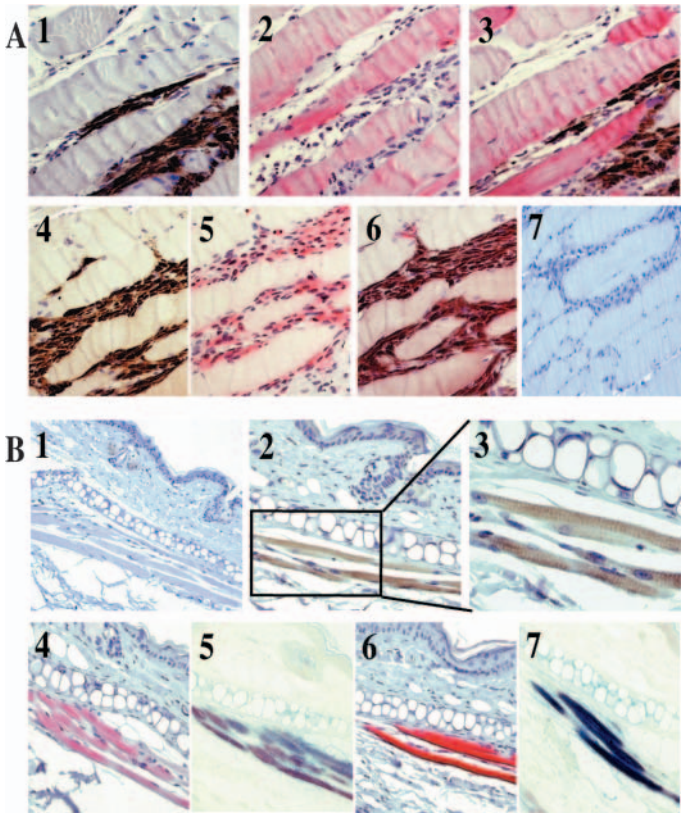

Fig. 6. Contribution of eGFP-MSCs into myofibroblast and myofiber-like cells in vivo. (A) eGFP positive cells with myofibroblast morphology were located among skeletal muscle fibers (A1,4; brown). No expression of desmin was observed (A2; red staining) showing mutual exclusion of expression when double staining for desmin and eGFP was performed (A3). These same eGFP$^+$ cells (brown) stained positive for α-sma (red) in serial sections (A5) resulting in a red-brown color. (A6) The same section stained for both rabbit and mouse immunoglubulins (isotype control) (A7). (B) Representative section of the skin from the ear with myofibers staining positive for eGFP (B2,3; brown cells). The same group of myofibers demonstrating expression of desmin (B4,5; pink-red staining) and FTM (B6,7; red) alone or in combination with an eGFP antibody (blue) giving a purple color (B5,7). Sections were counterstained with hematoxylin (except for B5,7). Magnifications: ×200 (A7, B1,2,4-7); ×400 (A1-6, B3).

Here, we report that a highly enriched muMSC population can be incorporated into several tissues after systemic infusion into recipient animals that only received sublethal irradiation. Our data indicate that infused MSCs can give rise to hepatocytes, renal tubular cells, bronchiolar epithelial cells, myofibers and myofibroblast-like cells, although at a low frequency. Different explanations could be proposed for the rare occurrence of these events. We chose to inject MSCs into recipient animals not forced to undergo severe organ degeneration and/or repair first. It is possible that injured tissues express specific receptors or ligands to facilitate trafficking, adhesion and infiltration of MSCs to the site of injury. Indeed, a recent report showed that muMSCs could differentiate into type II pneumocytes after systemic infusion in bleomycin-treated mice (Ortiz et al., 2003). The difference in the type of lung cells that MSCs differentiated into compared to our study can be justified either by the importance of specific tissue damage in promoting/enhancing this type of phenomena, or by the different experimental design used in our study. Although sublethal irradiation could incur some damage to the lungs, we believe that the physical retention of MSCs in this organ is a result of the large number of cells transplanted, or the fact that they weakly express appropriate adhesion molecules. As a consequence, this retention may have drastically reduced the number of potential MSCs capable of homing to other organs. These findings are in accordance with previous reports (Gao et al., 2001; Barbash et al., 2003). However, to our knowledge there are no reports on the potential detrimental effect that this retention of MSCs in the lung may cause on lung function. Thus, we suggest that systemic infusion might not be the best delivery route for this type of stem cell. In order to drive or enhance the homing and differentiation ability of the transplanted MSCs for tissue repair, specific or selective pressure may be required.

Again, the lack or weak expression of integrins and other adhesion molecules that play a vital role in cell migration and/or attachment to different tissues may also account for the inability of muMSCs to home back to the bone marrow. As reported recently, this loss and/or change in homing/attachment capacity of these cells could be due to the culture conditions used (Rombouts et al., 2003). Based on this fact, better understanding of the signaling mechanisms that attract bone marrow cells to specific tissues will be necessary in order to enhance the prospects of systemic delivery of MSCs as a therapeutic method for tissue repair. Local infusion of MSCs

to a tissue of interest might be an attractive alternative route of delivery.

Another possible explanation for the low frequency of the differentiation events seen here is that the MSC compartment is very heterogeneous and although we used an enriched MSC population, this may not have included the most primitive and possibly most multipotent cells. Recent findings from our group (Anjos-Afonso and Bonnet, 2003) indicate that MSCs contain a minor population of quiescent cells sharing some MAPC features (Jiang et al., 2002). Interestingly, despite the high transduction efficiency obtained with the lentivirus vector, we observed that the majority of this subpopulation of cells lay in the untransduced fraction (<2%). Therefore, cells with higher differentiation capacity might have unexpectedly been excluded from our experiment.

Finally, it is still unclear what mechanism is responsible for the observed differentiation phenomena shown in this study. Recent reports on the differentiation capacity of hematopoietic cells have identified fusion as the primary mechanism responsible for the observed phenomena (Terada et al., 2002; Ying et al., 2002; Alvarez-Dolado et al., 2003; Wang et al., 2003; Camargo et al., 2004; Willenbring et al., 2004). Although there are other mechanisms apart from fusion that have been shown to occur (Harris et al., 2004; Jang et al., 2004). The contribution of MSCs into different cell types reported here could have arisen from trans-differentiation, de-differentiation, fusion with resident cells or even a combination of these possible mechanisms. Although fusion is not the mechanism responsible for the in vitro differentiation capacity of muMSCs described here, we could not rule it out as a phenomenon occurring in vivo and in vitro, as recently described for hematopoietic cells (Alvarez-Dolado et al., 2003). It is possible that eGFP-MSCs that have been incorporated into the liver and the skin (myofibers) could have resulted from fusion. The main aim of this study was to address the 'natural' distribution of MSCs into different organs after systemic delivery, and possible in vivo contribution capacity of these cells. Due to the experimental design of this study we were unable to address the mechanism of these differentiation events but are currently dissecting the process leading to such phenomena.

In summary, we have shown that a defined, highly enriched muMSC population is capable of differentiating into various cell types when administered systemically under minimal damage conditions. Despite the low frequency of such phenomena, this observation demonstrates for the first time that muMSCs have multipotent capacities in vivo.

We thank all the staff from the histopathology unit for processing the tissues, especially George Elia for his technical advices. We also acknowledge Sam Janes and Andrew Nicholson for the lung pathology report. This work was supported by Cancer Research UK.

References

Alvarez-Dolado, M., Pardal, R., Garcia-Verdugo, J. M., Fike, J. R., Lee, H. O., Pfeffer, K., Lois, C., Morrison, S. J. and Alvarez-Buylla, A. (2003). Fusion of bone-marrow-derived cells with Purkinje neurons, cardiomyocytes and hepatocytes. *Nature* **425**, 968-973.

Anjos-Afonso, F. and Bonnet, D. (2003). Definition of a new hierarchy in the murine mesenchymal stem cell (muMSC) compartment with the identification and isolation of a quiescent sub-population expressing SSEA-1 antigen. *Blood* **112**, 415.

Baddoo, M., Hill, K., Wilkinson, R., Gaupp, D., Hughes, C., Kopen, G. C. and Phinney, D. G. (2003). Characterization of mesenchymal stem cells isolated from murine bone marrow by negative selection. *J. Cell. Biochem.* **89**, 1235-1249.

Barbash, I. M., Chouraqui, P., Baron, J., Feinberg, M. S., Etzion, S., Tessone, A., Miller, L., Guetta, E., Zipori, D., Kedes, L. H. et al. (2003). Systemic delivery of bone marrow-derived mesenchymal stem cells to the infarcted myocardium, feasibility, cell migration, and body distribution. *Circulation* **108**, 863-868.

Bartholomew, A., Patil, S., Mackay, A., Nelson, M., Buyaner, D., Hardy, W., Mosca, J., Sturgeon, C., Siatskas, M., Mahmud, N. et al. (2001). Baboon mesenchymal stem cells can be genetically modified to secrete human erythropoietin in vivo. *Hum. Gene Ther.* **12**, 1527-1541.

Bianco, P. and Robey, P. G. (2000) Marrow stromal stem cells. *J. Clin. Invest.* **105**, 1663-1668.

Bianco, P., Riminucci, M., Gronthos, S. and Robey, P. G. (2001). Bone marrow stromal stem cells, nature, biology, and potential applications. *Stem Cells* **19**, 180-192.

Brazelton, T. R., Nystrom, M. and Blau, H. M. (2003). Significant differences among skeletal muscles in the incorporation of bone marrow-derived cells. *Dev. Biol.* **262**, 64-74.

Camargo, F. D., Finegold, M. and Goodell, M. A. (2004). Hematopoietic myelomonocytic cells are the major source of hepatocyte fusion partners. *J. Clin. Invest.* **113**, 1266-1270.

De Bari, C., Dell'Accio, F., Vandenabeele, F., Vermeesch, J. R., Raymackers, J. M. and Luyten, F. P. (2003). Skeletal muscle repair by adult human mesenchymal stem cells from synovial membrane. *J. Cell Biol.* **160**, 909-918.

Deans, R. J. and Moseley, A. B. (2000). Mesenchymal stem cells, biology and potential clinical uses. *Exp. Hematol.* **28**, 875-884.

Demaison, C., Parsley, K., Brouns, G., Scherr, M., Battmer, K., Kinnon, C., Grez, M. and Thrasher, A. J. (2002). High-level transduction and gene expression in hematopoietic repopulating cells using a human immunodeficiency virus type 1-based lentiviral vector containing an internal spleen focus forming virus promoter. *Hum. Gene. Ther.* **13**, 803-813.

Devine, S. M., Cobbs, C., Jennings, M., Bartholomew, A. and Hoffman, R. (2003). Mesenchymal stem cells distribute to a wide range of tissues following systemic infusion into nonhuman primates. *Blood* **101**, 2999-3001.

Duan, H. F., Wu, C. T., Wu, D. L., Lu, Y., Liu, H. J., Ha, X. Q., Zhang, Q. W., Wang, H., Jia, X. X. and Wang, L. S. (2003). Treatment of myocardial ischemia with bone marrow-derived mesenchymal stem cells overexpressing hepatocyte growth factor. *Mol. Ther.* **8**, 467-474.

Gao, J., Dennis, J. E., Muzic, R. F., Lundberg, M. and Caplan, A. I. (2001). The dynamic in vivo distribution of bone marrow-derived mesenchymal stem cells after infusion. *Cells Tissues Organs* **169**, 12-20.

Gojo, S., Gojo, N., Takeda, Y., Mori, T., Abe, H., Kyo, S., Hata, J. and Umezawa, A. (2003). In vivo cardiovasculogenesis by direct injection of isolated adult mesenchymal stem cells. *Exp. Cell. Res.* **288**, 51-59.

Harris, R. G., Herzog, E. L., Bruscia, E. M., Grove, J. E, van Arnam, J. S. and Krause, D. S. (2004). Lack of a fusion requirement for development of bone marrow-derived epithelia. *Science* **305**, 90-93.

Hofstetter, C. P., Schwarz, E. J., Hess, D., Widenfalk, J., El Manira, A., Prockop, D. J. and Olson, L. (2002). Marrow stromal cells form guiding strands in the injured spinal cord and promote recovery. *Proc. Natl. Acad. Sci. USA* **99**, 2199-2204.

Jackson, K. A., Majka, S. M., Wang, H., Pocius, J., Hartley, C. J., Majesky, M. W., Entman, M. L., Michael, L. H., Hirschi, K. K. and Goodell, M. A. (2001). Regeneration of ischemic cardiac muscle and vascular endothelium by adult stem cells. *J. Clin. Invest.* **107**, 1355-1356.

Jang, Y. Y., Collector, M. I., Baylin, S. B., Diehl, A. M. and Sharkis, S. J. (2004). Hematopoietic stem cells convert into liver cells within days without fusion. *Nat. Cell Biol.* **6**, 532-539.

Jiang, Y., Jahagirdar, B. N., Reinhardt, R. L., Schwartz, R. E., Keene, C. D., Ortiz-Gonzalez, X. R., Reyes, M., Lenvik, T., Lund, T., Blackstad, M. et al. (2002). Pluripotency of mesenchymal stem cells derived from adult marrow. *Nature* **418**, 41-49.

Kale, S., Karihaloo, A., Clark, P. R., Kashgarian, M., Krause, D. S. and Cantley, L. G. (2003). Bone marrow stem cells contribute to repair of the ischemically injured renal tubule. *J. Clin. Invest.* **112**, 42-49.

Koc, O. N. and Lazarus, H. M. (2002). Mesenchymal stem cells, heading into the clinic. *Bone Marrow Transplant.* **27**, 235-239.

Kopen, G. C, Prockop, D. J. and Phinney, D. G. (1999). Marrow stromal cells migrate throughout forebrain and cerebellum, and they differentiate

into astrocytes after injection into neonatal mouse brains. *Proc. Natl. Acad. Sci. USA* **96**, 10711-10716.

Krause, D. S., Theise, N. D., Collector, M. I., Henegariu, O., Hwang, S., Gardner, R., Neutzel, S. and Sharkis, S. J. (2001). Multi-organ, multi-lineage engraftment by a single bone marrow-derived stem cell. *Cell* **105**, 369-377.

Lagasse, E., Connors, H., Al-Dhalimy, M., Reitsma, M., Dohse, M., Osborne, L., Wang, X., Finegold, M., Weissman, I. L. and Grompe, M. (2000). Purified hematopoietic stem cells can differentiate into hepatocytes in vivo. *Nat. Med.* **6**, 1229-1234.

Liechty, K. W., MacKenzie, T. C., Shaaban, A. F., Radu, A., Moseley, A. M., Deans, R., Marshak, D. R. and Flake, A. W. (2002). Human mesenchymal stem cells engraft and demonstrate site-specific differentiation after in utero transplantation in sheep. *Nat. Med*. **11**, 1282-1286.

Ortiz, L. A., Gambelli, F., McBride, C., Gaupp, D., Baddoo, M., Kaminski, N. and Phinney, D. G. (2003). Mesenchymal stem cell engraftment in lung is enhanced in response to bleomycin exposure and ameliorates its fibrotic effects. *Proc. Natl. Acad. Sci. USA* **14**, 8407-8211.

Peister, A., Mellad, J. A., Larson, B. L., Hall, B. M., Gibson, L. F. and Prockop, D. J. (2004). Adult stem cells from bone marrow (MSCs) isolated from different strains of inbred mice vary in surface epitopes, rates of proliferation, and differentiation potential. *Blood* **103**, 1662-1668.

Peled, A., Zipori, D., Abramsky, O., Ovadia, H. and Shezen, E. (1991). Expression of alpha-smooth muscle actin in murine bone marrow stromal cells. *Blood* **78**, 304-309.

Pereira, R. F., Halford, K. W., O'Hara, M. D., Leeper, D. B., Sokolov, B. P., Pollard, M. D., Bagasra, O. and Prockop, D. J. (1995). Cultured adherent cells from marrow can serve as long-lasting precursor cells for bone, cartilage, and lung in irradiated mice. *Proc. Natl. Acad. Sci. USA* **92**, 4857-4861.

Pereira, R. F., O'Hara, M. D., Laptev, A. V., Halford, K. W., Pollard, M. D., Class, R., Simon, D., Livezey, K. and Prockop, D. J. (1998). Marrow stromal cells as a source of progenitor cells for nonhematopoietic tissues in transgenic mice with a phenotype of osteogenesis imperfecta. *Proc. Natl. Acad. Sci. USA* **95**, 1142-1147.

Phinney, D. G., Kopen, G., Isaacson, R. L. and Prockop, D. J. (1999). Plastic adherent stromal cells from the bone marrow of commonly used strains of inbred mice, variations in yield, growth, and differentiation. *J. Cell. Biochem.* **72**, 570-585.

Pittenger, M. F., Mackay, A. M., Beck, S. C., Jaiswal, R. K., Douglas, R., Mosca, J. D., Moorman, M. A., Simonetti, D. W., Craig, S. and Marshak, D. R. (1999). Multilineage potential of adult human mesenchymal stem cells. *Science* **284**, 143-147.

Rombouts, W. J. C. and Ploemacher, R. E. (2003). Primary murine MSC show highly efficient homing to the bone marrow but lose homing ability following culture. *Leukemia* **17**, 160-170.

Terada, N., Hamazaki, T., Oka, M., Hoki, M., Mastalerz, D. M., Nakano, Y., Meyer, E. M., Morel, L., Petersen, B. E. and Scott, E. W. (2002). Bone marrow cells adopt the phenotype of other cells by spontaneous cell fusion. *Nature* **416**, 542-545.

Toma, C., Pittenger, M. F., Cahill, K. S., Byrne, B. and Kessler, P. D. (2002). Human mesenchymal stem cells differentiate to a cardiomyocyte phenotype in the adult murine heart. *Circulation* **105**, 93-98.

Wagers, A. J., Sherwood, R. I., Christensen, J. L. and Weissman, I. L. (2002). Little evidence for developmental plasticity of adult hematopoietic stem cells. *Science* **297**, 2256-2259.

Wakitani, S., Saito, T. and Caplan, A. I. (1995). Myogenic cells derived from rat bone marrow mesenchymal stem cells exposed to 5-azacytidine. *Muscle Nerve* **18**, 1417-1426.

Wang, X., Willenbring, H., Akkari, Y., Torimaru, Y., Foster, M., Al-Dhalimy, M., Lagasse, E., Finegold, M., Olson, S. and Grompe, M. (2003). Cell fusion is the principal source of bone-marrow-derived hepatocytes. *Nature* **422**, 897-901.

Willenbring, H., Bailey, A. S., Foster, M., Akkari, Y., Dorrell, C., Olson, S., Finegold, M., Fleming, W. H. and Grompe, M. (2004). Myelomonocytic cells are sufficient for therapeutic cell fusion in liver. *Nat. Med.* **10**, 744-748.

Woodbury, D., Schwarz, E. J., Prockop, D. J. and Black, I. B. (2000). Adult rat and human bone marrow stromal cells differentiate into neurons. *J. Neurosci. Res.* **61**, 364-370.

Ying, Q. L., Nichols, J., Evans, E. P. and Smith, A. G. (2002). Changing potency by spontaneous fusion. *Nature* **416**, 545-548.